An Update on Windows, Couplers, Higher-Order-Mode Damping, and Interlocks*

Larry Phillips

Continuous Electron Beam Accelerator Facility
12000 Jefferson Ave.
Newport News, VA 23606

I. Summary

One of the more consistently challenging problems associated with superconducting RF systems is the introduction of RF power to the cavity and the extraction of beam–induced high–order–mode power from the cavity. This usually involves the transmission of RF power between atmosphere and cavity vacuum spanning a substantial difference in temperature. Dielectric RF windows, usually ceramic, provide atmospheric barriers, and carefully designed thermal transitions of waveguide or coaxial line span the temperature difference while minimizing heat flow to the refrigeration system from conduction and RF losses.

There are exceptions, such as a proposed dual-beam accelerator in which RF power is generated in a parallel cavity structure which is RF coupled to accelerating cavities in a common vacuum environment.[1] Some machines such as the DARMSTADT linac do not generate enough higher order mode fields to disturb the beam and require no damping at all.[2] The CEBAF cavity, originally designed for higher current storage ring application at Cornell, generates only a few tenths of a watt with the CEBAF beam which is small enough to be economically dissipated at the cavity temperature and within the cavity vacuum envelope avoiding the need for a window.[3]

In general, this is not the case and larger values of higher order mode power must be dissipated at some intermediate shield temperature or outside of the cryostat at 300K. An example[4] is the HOM extraction system developed at KEK which is shown in Figure 1. The extraction of higher order mode power without

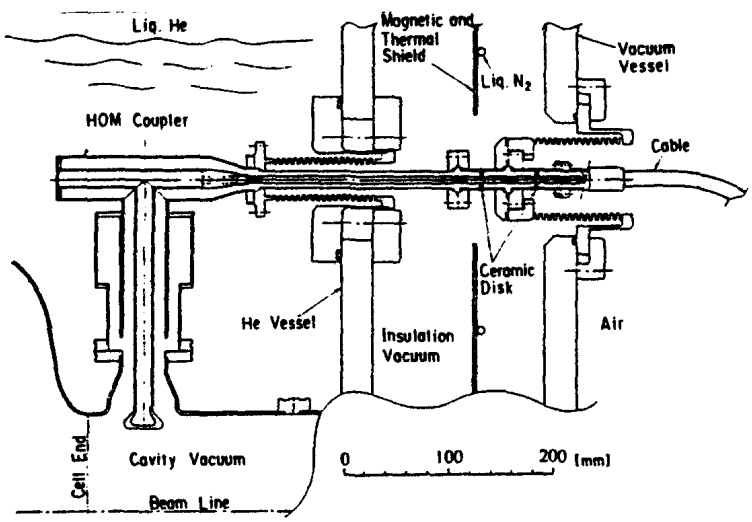

Figure 1. A coaxial higher order mode extraction system used at KEK (Ref. 4).

damping the fundamental accelerating mode of the cavity is accomplished by using a notch filter between the coupling probe and the load. Common to all HOM damping systems is some method of rejecting the fundamental mode. In some cases adequate HOM damping is achieved using an array of probes which do not couple to the fundamental frequency avoiding the need for rejection filters.[5] Waveguide HOM couplers offer a simple method of rejecting the fundamental mode of the cavity by choosing the cutoff frequency of the HOM waveguide slightly above the fundamental frequency. One drawback of this system is that it is not as sharp as a tuned filter, and modes close to the fundamental are also rejected. In this case they must damped instead through the fundamental power coupler.[6] This complicates the fundamental power coupler somewhat by requiring it to have a greater bandwidth than would otherwise be necessary. The large physical size of waveguide couplers at the lower frequencies can be a significant drawback.

Another technique being developed for B-factory cavities provides HOM damping at 300K by placing RF absorbing tiles in the cavity vacuum on the inside of the beam pipe which is large enough for the modes to propagate.[7] The tiles are separated from the cavity by a special section of beam pipe designed to allow higher order modes to propagate while blocking the fundamental mode.

An example of a coaxial fundamental power coupler is the 500 MHz HERA coupler[8] shown in Figure 2. This design uses one cylindrical RF window at 300 K as part of a

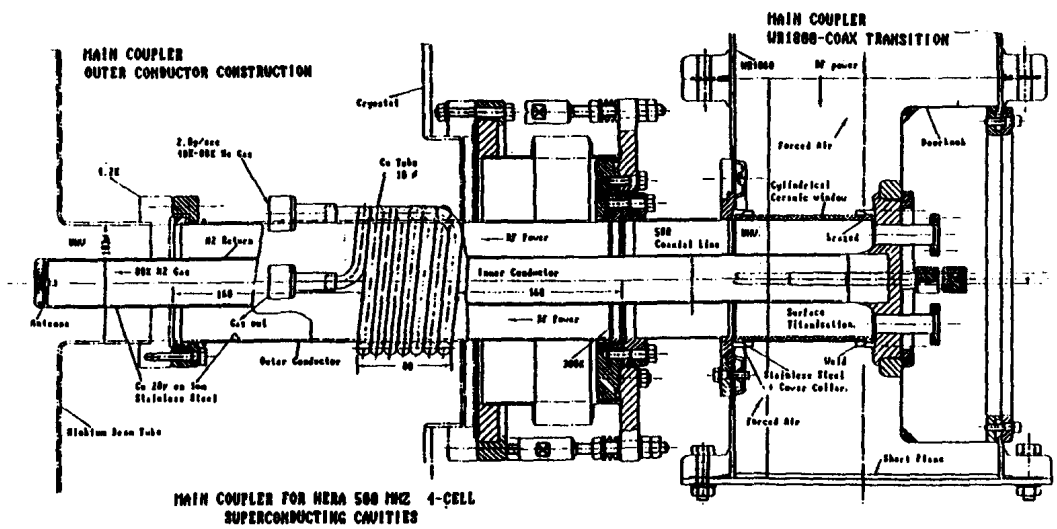

Figure 2. Reference 8.

waveguide to coax transition which extends the cavity vacuum to include warm coupler surfaces. An alternate method is to use one cold window and a second window at 300 K. The cold window can serve as an additional barrier to protect the cavity from outgassing from warm surfaces and the introduction of debris during assembly, but on the other hand can also be exposed to greater levels of cavity-induced radiation. Both single—and double—window couplers are in use, and the relative advantages of each are not entirely clear at present. Although this coupler is fixed, coaxial couplers lend themselves more readily to variable coupling over a wide range by incorporating variable probe penetration into the design. With respect to this feature, waveguide couplers appear to have a disadvantage. The HERA coupler also contains a light detector and an electron probe

close to the window for diagnostic and interlock purposes should arcing or multipacting occur. Similar devices are used on most medium and high power couplers and are considered essential in order to avoid damage to the coupler or to the machine. The need for these devices is due to a variety of electronic processes occurring at window and coupler surfaces. These processes are still a major problem with RF windows and couplers and have been responsible for much damage and lost beam-time. With respect to these processes, coupler and RF window performance is not well-understood, in the sense that reliable designs with predictable performance are not currently available. The design of these components has not yet been reduced to standard engineering practice. This is not true of most other SRF components with the exception of cavities. Both cavities and couplers (including windows) have a high sensitivity to surface conditions and minute defects which are hard to control. Aside from cavities, windows are probably the most sensitive and problematic components of the cavity/cryostat system. They are prone to multipacting and arcing which interferes with the transmission of RF power and occasionally damages a window, venting a cavity to air. The use of fast interlocks in the window, region is known to reduce the likelihood of such failure and is common on most machines. Although the number of interlock trips and window failures experienced may be tolerable for existing machines with current window designs, it would seem that future accelerators, with perhaps several orders of magnitude more windows involved, would require a greater level of performance predictability.

A better understanding of window and coupler performance can be obtained by examining the operational history of these components in existing accelerators. Consequently, part of this work will contain a discussion of window breakdown phenomena and a review of coupler performance in a sampling of existing machines. Since these phenomena are highly dependent on materials and surface properties, a review of these topics is also included.

II. Types of Window Breakdown

It is often noticed that RF windows exhibit breakdown at much lower voltages than comparable insulators in DC fields. A typical DC breakdown example as depicted by Latham[9] is shown in Figure 3.

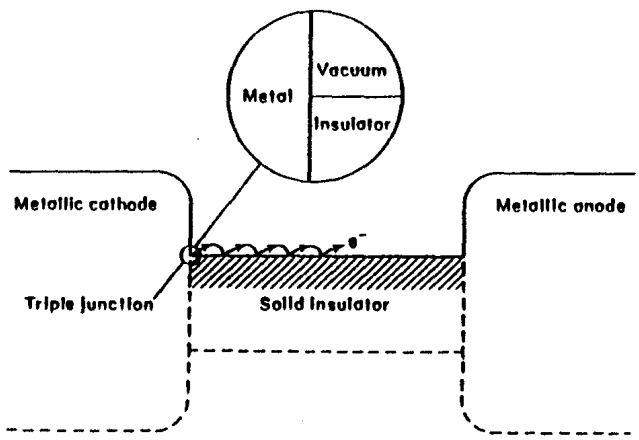

Figure 3. A typical high voltage breakdown process for an insulator in vacuum after Latham (Ref. 9.)

Here "breakdown" is used to mean arcing, surface flashover, or any process producing either light or electrons. It is interesting to compare the processes leading to breakdown in each case. At low fields, stray electrons from natural background sources are swept out of the gap uneventfully. At sufficiently high fields, electron emission from the cathode metal-vacuum-ceramic interface ("triple junction") occurs. Some of the emitted electron current will strike the ceramic surface, producing many more free electrons since the secondary electron emission (SEE) coefficient is high for most ceramics (typically 6 to 10 for alumina). This will leave the ceramic surface positively charged near the cathode, increasing the electric field near the triple junction and further increasing the field emitted current leading to breakdown.

RF window breakdown can be stimulated by processes local to the window, such as multipacting, or by processes related to the cavity environment. RF breakdown associated with multipacting can occur at any RF field level for which resonant electron trajectories exist that end on surfaces with SEE coefficient greater than one. Stray electrons from natural background sources in this case can find their way into such trajectories in which electron multiplication can take place, ultimately producing a swarm of electrons traversing the path between the endpoints of the trajectory synchronous with the RF field. Common to both RF and DC breakdown processes is an electron multiplication enhanced by high secondary electron emission yields of the relevant surfaces.

Other sources of electrons from the cavity environment can stimulate electronic activity at the window. Field emitted electrons emanating from the cavity can, in some geometries, strike the window or surfaces near the window.[10] X-rays generated by field emission in the cavity can also produce free electrons at the window by photoemission or Compton scattering. X-rays of energies substantially attenuated by the window material can, by photoemission, produce differential charging of inner and outer surfaces of the window.

It has also been shown that electrons can be driven down a waveguide coupler as an "electron wind" in the direction of RF power flow by a multipacting process which translates down the coupler.[11] Since there is usually some level of x-ray flux permeating coupler surfaces upstream of the window, this would imply an additional electron source for the inner window in two window systems with an intervening vacuum space.

Environmental effects in most cases go unnoticed unless they are discovered by accident. This was case for SLAC klystron windows which were observed to suffer more failures in service on klystrons than from comparable service in test rings.[12] Similarly, considerable electronic activity and arcing was observed from the CEBAF window during operation on the cavity.[13] This activity was seen to be absent when the window was operated in waveguide test resonator without field emission present. The CEBAF window is an extreme example in which all electronic activity appears to be due to the cavity environment.

In addition to electron loading of the RF field in the coupler, multipacting can produce window heating and surface charging. There are several forms of permanent damage which are commonly associated with these effects, such as punctures and thermal stress cracking. Localized multipacting at surface defects is thought to cause window punctures initiating at the surface by localized heating and then branching out through the bulk. A typical puncture of this type is shown in cross-section by Saito,[14] et al. as seen in Figure 4. The initial puncture site on the left edge of the window is seen to propagate

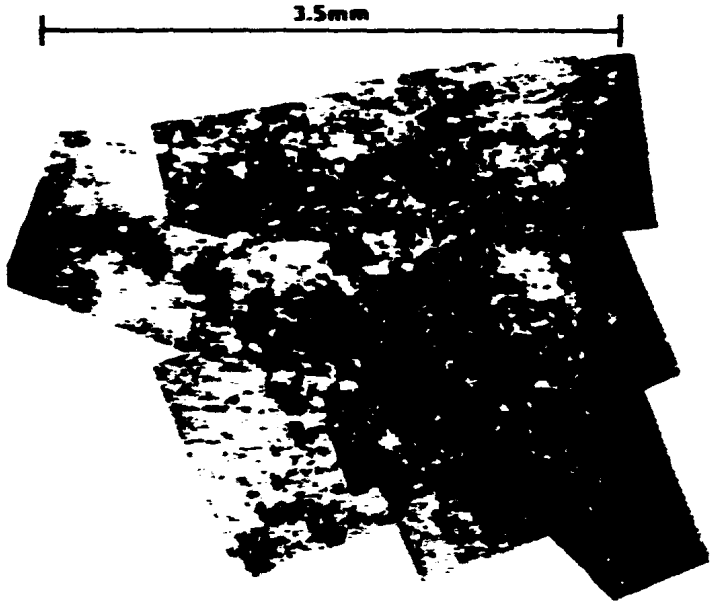

Figure 4.

through the entire thickness of the window (3.5 mm) with branching cracks emerging on the opposite face. A somewhat different type of puncture[15] is shown in Fig. 5- This type

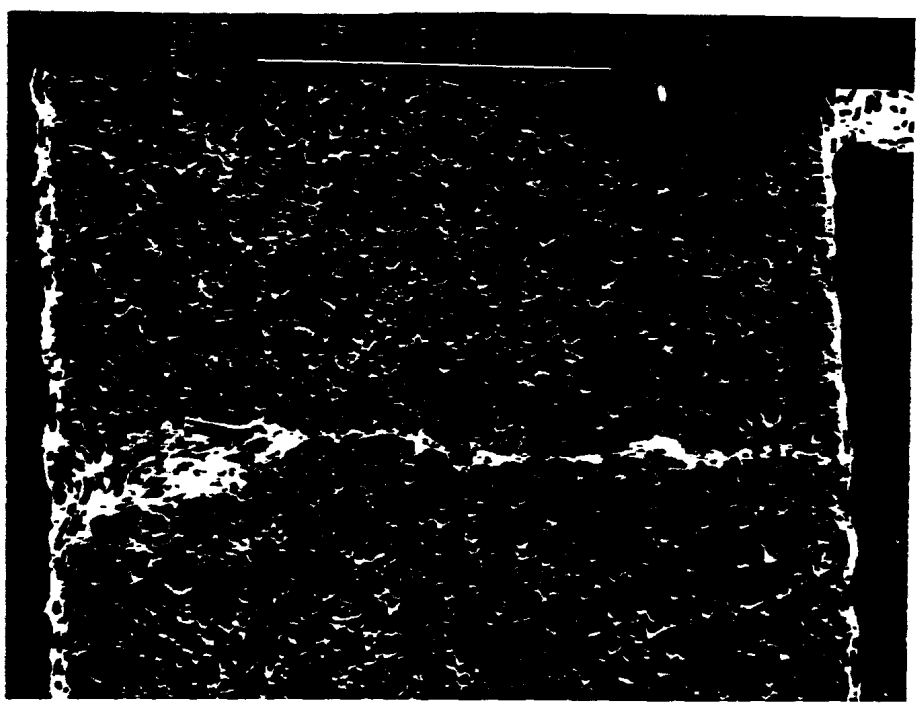

Figure 5. A CEBAF RF window "puncture" through aluminum oxide ceramic. (Ref. 15).

of puncture occurs in CEBAF windows during operation in which no signs of multipacting are apparent. A narrow channel extends completely through the 1 mm thick

aluminum oxide ceramic without the lateral branching seen in Fig. 4. There are also no signs of surface melting at the end of the channel. The channel emerges from each side of the ceramic, as a nearly round hole and not a crack. It is known that the CEBAF window becomes charged by electrons from the cavity environment when operating with field emission as will be described later. It is assumed that this puncture is produced by an electrical breakdown of the ceramic due to surface charging. The maximum difference of potential which can be developed across the ceramic through surface charging will depend on the mechanism producing the surface charge. In the case of localized multipacting at some point on the ceramic surface, it would seem that the maximum voltage is limited by the peak RF voltage at the window. In the case of window charging resulting from exposure to the cavity environment, the maximum D.C. window potential is limited to the energies of the electrons or x-rays emitted from the cavity. Breakdown strengths for electronic ceramics commonly used for RF windows are typically on the order of 25 kV/mm in the absence of radiation. The 10 mm thick coaxial window used in TRISTAN has also experienced punctures and is operated at relatively low rf voltages and without substantial field emission in the cavity. The nature of this form of window damage is not yet well understood.

Another form of RF window damage results from thermally induced mechanical stresses from localized heating of the ceramic. Such heating is frequently produced by metal films deposited on the ceramic surface by "RF sputtering" from adjacent metal surfaces. The films become conducting and absorb power from the RF field. Although commonly referred to as "RF sputtering", the actual process of metal transfer is also not well understood. The surface from which metal is removed may appear textured unlike the target erosion seen on a conventional RF sputter target. Early CESR windows which had failed by this process showed short narrow arc trails about one mm wide and 10 or 20 times as long following an erratic path on the surface of a copper corona ring adjacent to the deposited copper film. Windows from TRISTAN which have failed by this process show an "orange-peel" texture on the adjacent copper surfaces.[16]

It is generally believed that this process is probably connected with, or perhaps initiated by multipacting which is known to release large quantities of gas from the surface through electron stimulated desorption. Once an ionized cluster of gas and metal vapor is formed at a surface at high RF field levels, a continued local absorption of RF power in the cluster can continue to vaporize more copper into the arc. Localized copper deposition on a TRISTAN window[17] ceramic is shown in Fig. 6. The most common

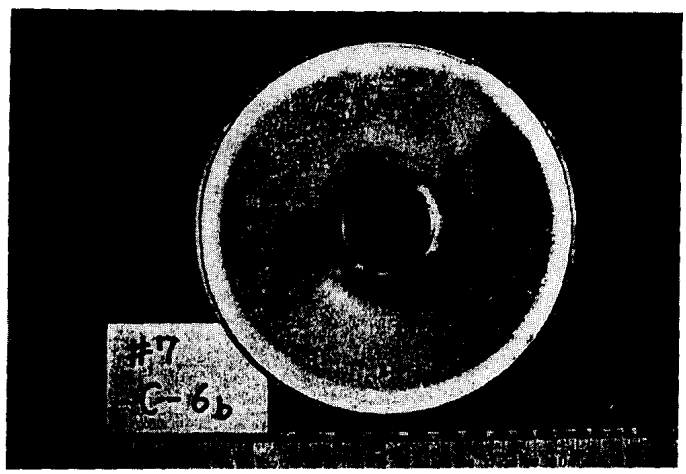

Figure 6. A failed window with copper sputtered on portions of the surface. (Ref. 17).

precaution taken to avoid this problem is to maintain the vacuum at the window to approximately 10^{-7} Torr or better, and to provide a fast shutdown of RF power when a gas burst or multipacting is sensed at the window. Altering the window geometry is another alternative, which proved effective for the CESR window problem, where the high fields were due to HOM resonances at the window.

III. Operational History of Windows and Couplers in Existing Machines

A summary of coupler types for a number of existing accelerators is given in Figure 7.. Performance limitations of windows and couplers still have a significant impact on the operation of most accelerators. This is not true for machines operating at very low RF power levels. The s-band coupler used in the linac at Darmstadt operates at power levels under 500 watts. For this system, no window problems are seen and window interlocks are unnecessary. Over the life of the machine a few window ceramics have been broken through mechanical means not related to machine operation.

Machine	S-DALINAC	HEPL	CEBAF	HERA	LEP	TRISTAN
Frequency	3 Ghz	1.3 Ghz	1.5 Ghz	500 Mhz	352 Mhz	508 Mhz
RF power per coupler	0.5 kW	10 kW	4 kW	100 kW 300 kW traveling wave	40 kW 180 kW traveling wave	75 kW 200 kW traveling wave
Coupler Type	Coaxial with Planar window	Coaxial with Cylindrical window	Waveguide with Planar window	Coaxial with cylindrical window	Coaxial with cylindrical window	Coaxial with Planar window
Coupling Range, Qext	Fixed ↓ variable 10^7-10^{10}	Variable	Fixed	Fixed-slightly adj. with external tuning stubs	Fixed ↓ variable 5×10^5 - 3×10^9	Fixed
Window Temp.	300 K 2 K	300 K 77 K	300 K 2 K	300 K	300 K	300 k

Figure 7. A sampling of some fundamental power coupler characteristics.

A similar situation exists for the HEPL linac which has the longest history of operation of any superconducting accelerator. It operates at 1.3 Ghz with a maximum input coupler power of 10 kW. Over the life of the machine there have been some window failures attributed to age and thermal cycling but no RF-related failures. Window interlocks are not used and no signs of coupler multipacting or other electronic activity are apparent.

The CEBAF input coupler operates at 1.5 Ghz with a forward power of up to 4 kW. Unlike the HEPL and DARMSTADT couplers, it experiences a wide variety of electronic activity but only in the presence of field emission in the cavity. This activity appears to be entirely caused by the cavity environment, and, when the window is operated in a test resonator or with the cavity detuned, it is entirely absent regardless of RF power levels at the window. The difference is quite dramatic and strongly indicates x-rays or electrons impinging on the window produced by field emission in the cavity as suggested by Sundelin.[18] A subsequent series of tests[19] using an insulated window to measure electron or photoelectron current to or from the window verified the existence of such current and measured its dependence on field emission as shown in Fig. 8.

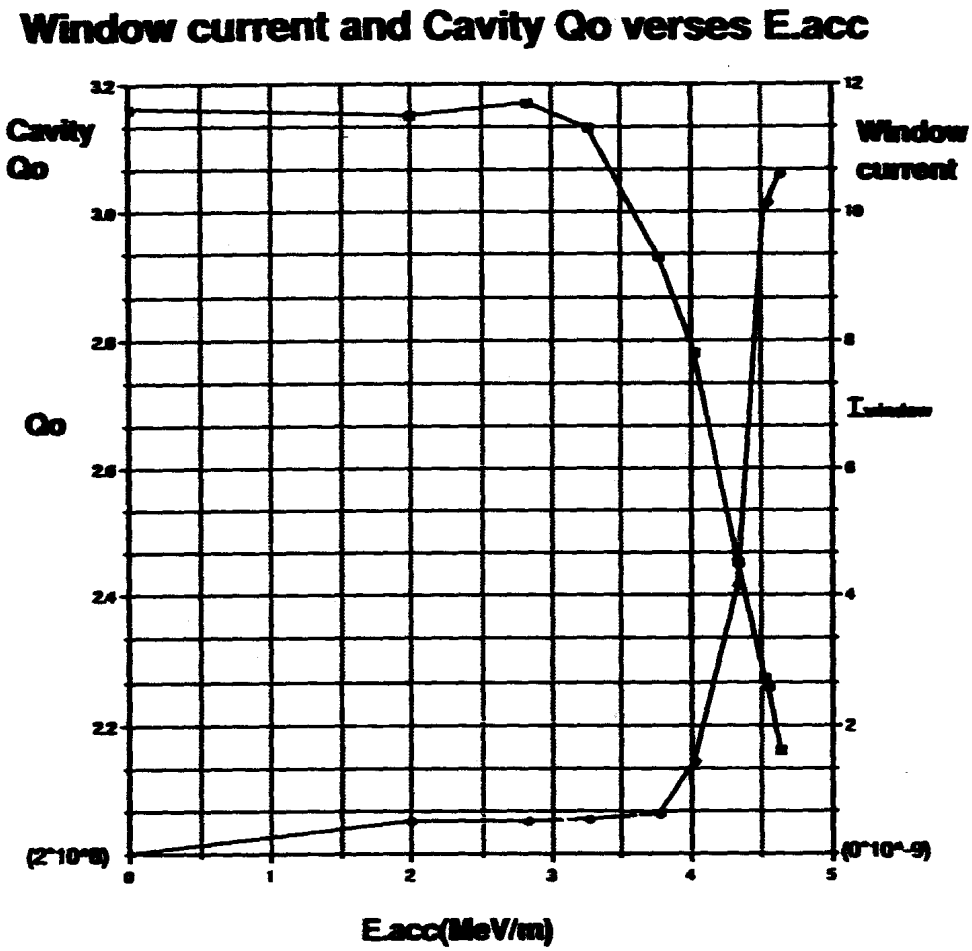

Figure 8. Current collected on an electrically insulated cold RF window compared with cavity Q degradation from field emmission (Ref. 19).

The effects of field emission in the cavity on window arcing were studied in a separate series of tests using a standard CEBAF production cavity which was specially instrumented for the purpose. Four parameters were recorded simultaneously when an arc occurred: reflected power (Pref), transmitted power from the cavity field probe (P_{trans}), photomultiplier tube output (PMT recording light from window region), and the output of an x-ray detector placed near the window (radiation diode). The four channel

recording is triggered either by a PMT signal or a change in the reflected power signal. A typical event in which all four parameters are involved is shown in Figure 9.

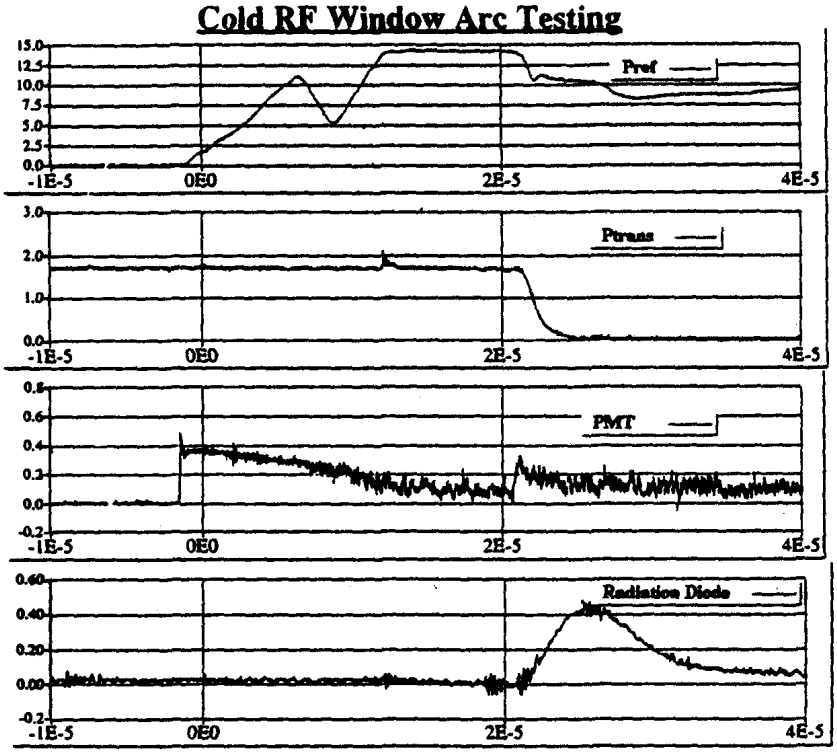

Figure 9. One type of CEBAF cold window "arc" producing transients in reflected power, transmitted power, window light (PMT), and radiation near the window (Ref. 20).

An interesting feature of this event is seen in the rapid decay of the transmitted power signal occurring more than 20 μsec after the trigger. The decay time is too small for any external damping mechanism and is attributed to a swarm of electrons produced in the cavity by the window arc rapidly dissipating the cavity field energy. This interpretation is supported by the existence of a strong x-ray pulse which always appears with this type of fast quench (the bandwidth of the radiation channel is much smaller that of the transmitted power channel) as seen in the last trace. These phenomena have been described in detail in a recent publication[20] as well as in a paper in these proceedings.[21]

As mentioned earlier, punctures occur in a few percent of CEBAF windows tested (see Figure 5). These punctures show up after vertical cavity pair testing and are typically produced by cavities with poor performance in which the onset of field emission occurs at low fields (4-6 MV/m). It is assumed that the windows are subject to heavy differential charging under these conditions, leading to electrical breakdown through the ceramic. Breakdown occurs preferentially in any one of four corners of the window. Such a site preference is consistent with breakdown from charging unless there were some other pre-existing defects in these locations. To test this, windows were coated on both sides with sputtered copper films and then attached to a high voltage source to produce punctures.

Under these conditions the punctures were randomly located indicating that punctures are produced by a preferential distribution of surface charge rather than a preferential distribution of weak spots in the ceramics.[22]

The HERA coupler which is very similar in design to the CERN coupler operates at 500 Mhz up to 100 kW. In approximately 2 years of operation no windows have been broken. The major operational problems experienced are related to the existence of multipacting barriers and the effort needed to condition them. Conditioning can take up to several weeks before stable operation is achieved. In addition, conditioning does not last, and with time the same multipacting barriers reappear and reconditioning becomes necessary. This can occur within 6 to 8 weeks. When the machine is in standby, the RF drive is ramped up and down to keep couplers conditioned. While processing through a multipacting barrier, light, gas bursts, and electrons collected on a pickup probe next to the window are observed. Light in the form of a stable glow has also been seen in the space between the inner and outer conductors. Running the RF drive ± 10" off cavity resonance is also found to be beneficial during conditioning.

The conditioning and deconditioning behavior of the coupler is consistent with long term gas migration and electron-induced gas desorption of the coupler surfaces by the multipacting process. It is known that this process reduces the secondary electron emission coefficient of surfaces, also consistent with the temporary elimination of a multipacting barrier by conditioning.

Similar conditioning and deconditioning effects are seen at CERN and elaborate conditioning procedures have been found useful. Couplers are conditioned on a warm test stand before being installed on cavities. It is quite interesting that in transferring the conditioned coupler from test stand to cavity, the coupler remains conditioned even after an exposure of 1/2 hour to room air. It is also observed that the deconditioning effect seems worse when the coupler is on the cavity than on the test stand.

Although some shadowing has been seen on a few ceramics, there have been no windows broken in operation on the superconducting cavities in LEP. Ten windows have been broken on copper cavities, the reasons for which are not clear.

The same effects of conditioning and deconditioning are also seen at KEK with the TRISTAN coupler. A procedure has been developed for conditioning the coupler on the cavity with the cavity warm. This has proven very successful and is considered essential for effective conditioning.[23]

It is also interesting in terms of gas migration that deconditioning is first seen in couplers on cavities next to the warm arcs. Common to all three couplers at LEP, HERA, and TRISTAN, is that the cavity vacuum is exposed to a warm window at 300 K and coupler surfaces through a thermal transition to 300 K.

The TRISTAN window is a coaxial ceramic disk 10 mm thick. In the period up until the beginning of '92 some window damage had occurred. Several windows had been punctured and several had been cracked from sputtered copper on the ceramic. Since that time, titanium nitride coatings and arc detectors have been used on all windows. There have been no subsequent RF related failures.

IV. Coupler Performance, Materials, and Surfaces

Two major factors limiting coupler performance are multipacting and radiation from the cavity. Performance with respect to multipacting is determined by the geometry of coupler surfaces as well as the physical and electronic properties of coupler surfaces. The secondary electron emission coefficient of the surface depends on material, its surface texture, the energy and angle of the incident electron, and the nature of the adsorbed gas layer.

Multipacting requires the existence of resonant electron trajectories between one or more points on the coupler surface having SEE coefficients, or their product, greater than unity at the electron energies relevant to the trajectory. If for a given distribution of secondary electron emission coefficients over a coupler surface, the coupler geometry did not contain such trajectories, multipacting would be eliminated. Also, if the SEE coefficient of all coupler surfaces could be reduced below unity, multipacting would be eliminated regardless of the geometry. Traditionally, both approaches have been used to suppress multipacting. The fact that multipacting is still a problem is probably due to the fact that the SEE coefficients of surfaces are not well known in the accelerator environment.

The influence of geometry on multipacting in RF structures has been studied using computer programs which calculate resonant electron trajectories.[24] To be fully accurate for window structures, such programs would have to account for both standing wave and traveling wave power in the coupler and incorporate the growing DC electric fields from window charging as multipacting progresses and reincorporate them into the trajectory calculation. Apparently none of the existing programs include all these all features. In a recent study on S–band pill box window, a computer simulation of multipacting on the ceramic disk agreed quite well with spatial patterns of light emitted from the disk as a function of RF power level.[25] Also confirmed was the predicted disappearance of multipacting above 50 MV/m. At yet higher fields the dominant cause of window failure was attributed to bulk defects in the ceramic in the form of voids.

One method employed to reduce or eliminate multipacting where possible is to control the secondary electron emission coefficient of surfaces through the use of special coatings. Such coatings are commonly used on ceramic window materials but are rarely used on surrounding metal surfaces, even though these surfaces frequently participate in multipacting. One problem connected with their use is the fact that they are not really well understood both in terms of producing the coatings as well as how they function in an accelerator environment. This is suggested by the fact that the recipe for these coatings is different at various laboratories even though the same problem is being treated. Such coatings are frequently titanium or titanium compounds.[26,27,28]

Secondary electron emission coefficient measurements of anti-multipacting coatings on ceramic surfaces are quite difficult and very few studies have been made characterizing their composition and performance.[29] In a recent study, Michizono and collaborators[30] examined the dependence of the secondary electron emission coefficient of titanium nitride films on alumina substrates as a function of film thickness, (Figure 10). In the same work they also examined the RF loss due to these films as a function of film thickness using window heating measurements (Figure 11). The results indicate that a balance must be chosen between increasing SEE for thin films and excessive film heating for thick films. The sharp increase in RF dissipation with thickness prevents the use of very thick films for which the SEE has saturated, but the combined results show a range from one to two nanometers where a good compromise is obtained. This optimum is

good for the substrate material and roughness used in this experiment and may need to be reexamined for other situations.

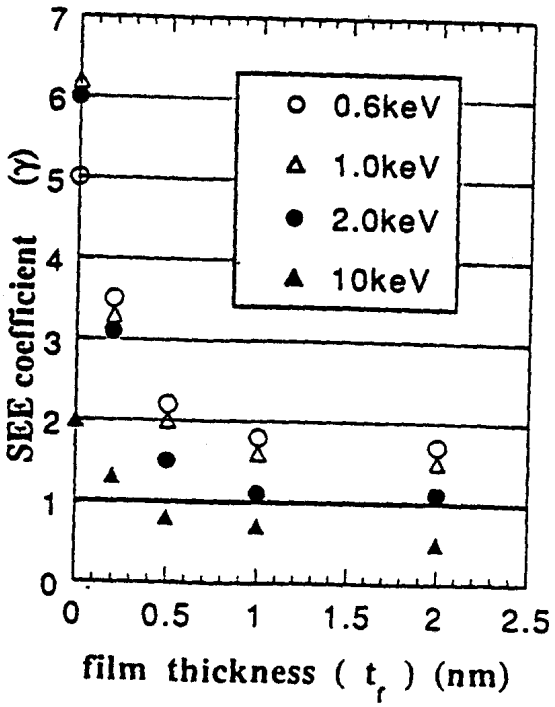

Figure 10. The dependence of secondary electron emission coefficients of TiN films as a function of their thickness as deposited on alumina substiate (Ref. 28).

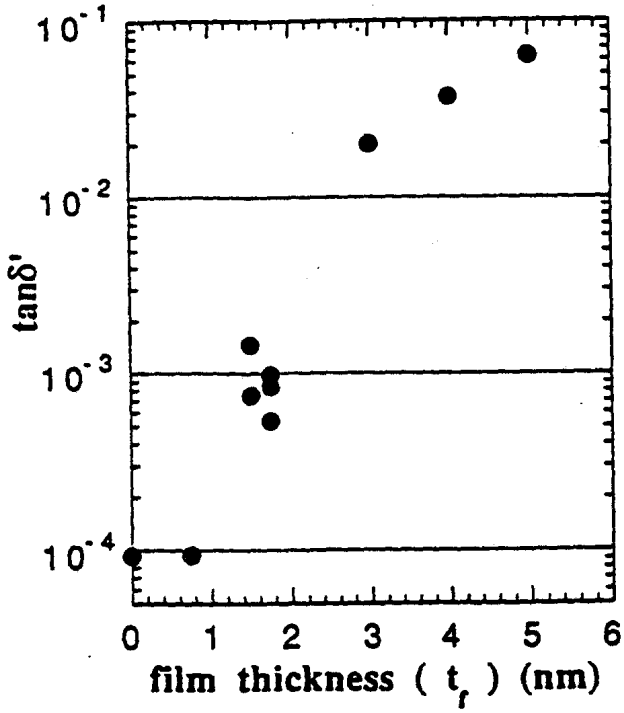

Figure 11. Effective dielectric loss tangents of alumina ceramics coated with TiN films (Ref. 28).

To further examine the effectiveness of the films under real conditions, a window (circular pillbox geometry) was coated in each of four quadrants with films of thicknesses from 0.5 to 2.0 nanometers. During RF operation multipacting was observed optically in the 0.5 nanometer quadrant with the others remaining relatively dark. An optimum thickness of 1.5 nanometer was chosen in this work.

Another interesting effect which was observed in this study, was the disappearance of excess titanium nitride for films in excess of 1.5 nanometers in as little as one week of high power operation. This was attributed to possible surface melting by the authors. A similar effect was seen[31] on the coupling slots in SPEAR cavities at SLAC some years ago. Approximately 20 nanometers of TiN was routinely deposited on the metal coupling slot surfaces to avoid multipacting and the coating would routinely disappear after several years of operation. In this case the mechanism was not established.

The build up of DC fields on window-ceramics from surface charging is in general not well understood. In some cases, mechanisms have been identified. Electrons and x-rays from the cavity appear to be the primary source for CEBAF windows.[32] Surface charging by localized multipacting at surface defects becomes a major problem for high power windows.[33,34] This is generally attributed to runaway heating at defect sites. Presumably, the antimultipacting coating is also defective at such sites, which enables

multipacting to initiate. In some cases, surface flashover results from surface charging on TiN-coated windows without any evidence of multipacting as seen in a study by Y. Saito, et al.[35] In this work a retractable probe was used to measure the state of surface charge on the window before and after surface flashover. Apparently the TiN coating on these windows did not supply charge drainage.

In principle, some charge drainage can be supplied by antimultipacting coatings which are partially conducting, but some balance between tolerable film heating and charge drainage is required.[36,37] This is aggravated by the fact that deposited films first form a discontinuous island structure which provides substantial RF loss even without charge drainage. At greater film thicknesses these films become globally conducting and additional RF loss is produced. This can be seen as a highly non linear RF loss with film thickness[38] (Figure 11).

Obtaining the proper film thickness for such films becomes quite critical. Further complicating the issue is the fact that the optimum thickness is not predictable since the value at which charge drainage occurs very much depends on substrate roughness and deposition conditions.

Several recent efforts may offer an alternate way of providing charge drainage. At CEBAF, very thick oxides are made partially conducting by doping them with metallic impurities during deposition by ion-beam sputtering from a composite metal/oxide target of an oxide having a low SEE coefficient.[39] Films having a nearly linear dependence of surface conductance with film thickness and very high bulk resistivities have been achieved (Figure 12).

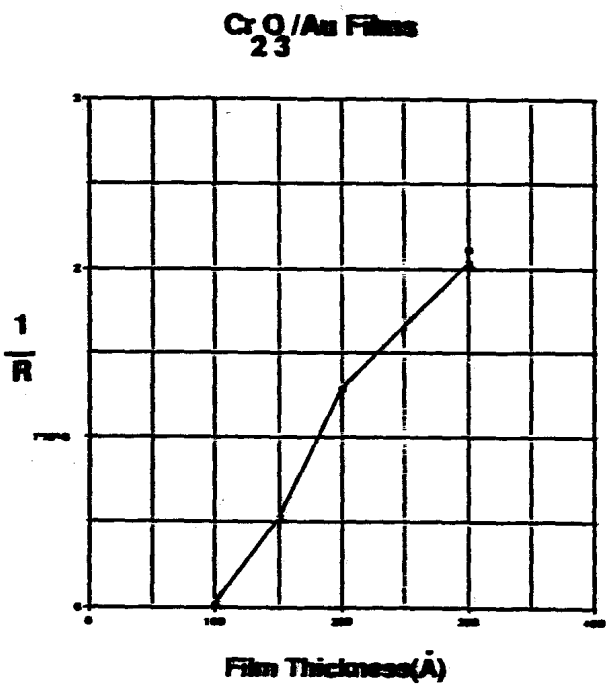

Figure 12. The sheet conductance of relatively thick films of chrome oxide co-sputtered with gold (Ref. 39).

Another approach by A Simone and coworkers at Lawrence Berkeley Laboratory provides a thin conducting layer by ion implantation of metallic impurities into the surface of ceramic.[40] A surface resistance of 10^{10} ohms/square was achieved on an alumina cylinder using titanium ions penetrating to a depth of approximately 1500 A.

A totally different approach to lowering the SEE coefficient of surfaces is by altering their geometry in an appropriate way using grooves or extremely rough surfaces. Although this is an old technique, it deserves to be revisited. On a macroscopic scale, surface grooves have been used successfully in the past to suppress multipacting both on metal surfaces and on ceramic windows.

An extensive study on window multipacting was carried out in which a variety of window coatings and surface grooving were compared in high power resonant ring tests at S-band.[41] A pill box window geometry was used to compare alumina, beryllia and silica discs three inches in diameter along with antimultipacting coatings of titanium and its oxides, and silicon oxide. Coatings alone could not completely eliminate multipacting. Grooved surfaces were also explored (Figure 13).

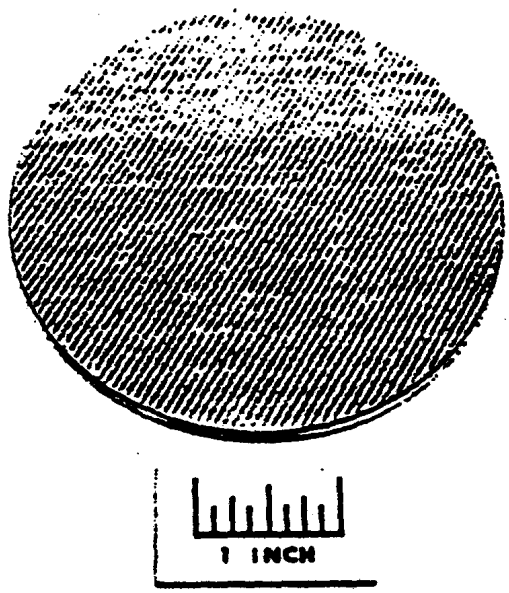

Figure 13. S-band grooved beryllia disc (Ref. 41).

Grooves were found to be relatively effective when oriented perpendicular to the electric field and ineffective when parallel, but when used alone, they also did not completely eliminate multipacting. When the grooved surface was also coated with titanium monoxide, multipacting was completely suppressed up to 85 megawatts which was the limiting power for the resonant ring. Since the secondary electron emission coefficient increases for impact at glancing angles, and the RF field is parallel to the surface, grooves have an increased effectiveness when perpendicular to the field. In this work, the only grooves studied were triangular and relatively shallow, and, as the authors point out, variations on this approach may provide a more efficient means of multipactor suppression. They further remark that "the method has the advantage of not being subject to changes when exposed to various atmospheres..." at least to the extent that the suppression is, in part, geometrical.

Before the advent of spherical and elliptical cavities, multipacting was a serious limitation to cavity performance. At that time the use of grooves on metal cavity surfaces to suppress multipacting was explored at HEPL and also at Cornell[42] with some limited success.

This work, both on grooved window ceramics and on metal surfaces, was done at a time when the current techniques of fine pattern formation and trenching using lithography and plasma chemistry were not available.

Another process for lowering the SEE coefficients of metal surfaces arises from the fact that the soot formed by the metal can have a much lower value than that of the metal itself.[43] The values for nickel soot and smooth nickel are compared in Figure 14. Soots can be produced for many metals by evaporating the metal in argon at about 1 Torr or so such that substantial deposition occurs, but many metal-metal collisions occur in transit, and much clustering occurs in the process. Some structural integrity can be imparted to the soot by some sintering at the expense of a slight rise in the SEE coefficient. By combining soots with grooves, values as low as 0.23 have been achieved.[44]

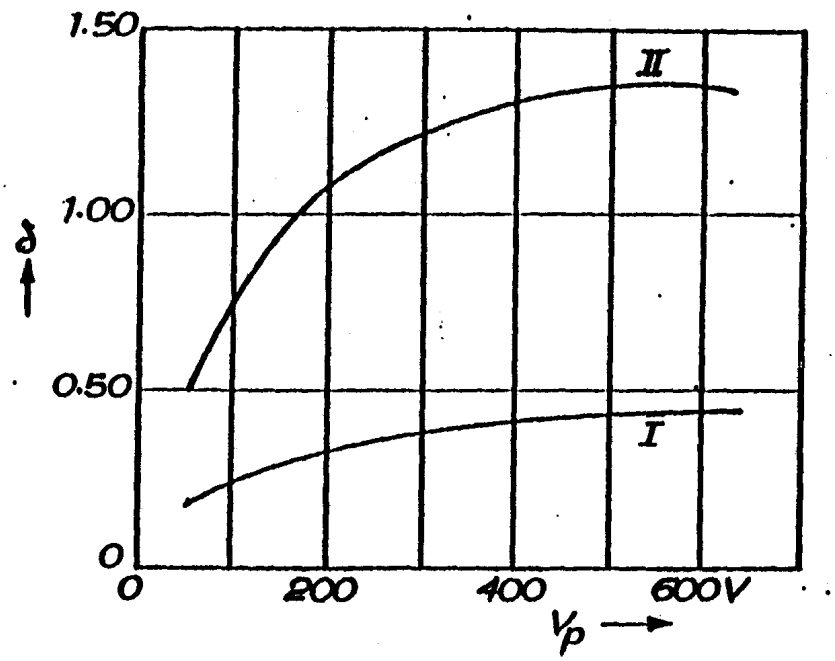

Figure 14. Secondary electron emission coefficients of a nickel plate (II) and nickel soot (I), after Brining (Ref. 43).

An interesting question is how such surfaces behave in accelerator environments and what is the influence of conditioning by multipacting on the secondary electron emission coefficient.

These questions were examined for a limited number of materials and conditions by M. Laverec and coworkers by measuring the variation of the SEE coefficient with exposure to electron bombardment.[45] The technique involved measuring the secondary electron emission coefficient of real surfaces containing adsorbed gases and other contaminants as

they might occur in an accelerator environment. A stationary electron beam was focused to a spot on a metal surface and the variation of the SEE coefficient with time was measured. In general a decrease in the SEE coefficient is seen with increasing electron dose saturating at some value. To show that this change was due to electron bombardment, the beam was swept back and forth across the exposed spot resulting in an increase in SEE to the initial value on either side of the spot. The effect of a 2 mm diameter electron beam focused on a spot on the surface of a smooth gold film for 100 minutes is shown in Figure 15. The effect of electron irradiation with time on gold soot ("gold black") is shown in Figure 16. These results are entirely consistent with the processing of surfaces at multipacting barriers. A deconditioning was also shown to occur for surfaces sitting idle for a long time in vacuum.

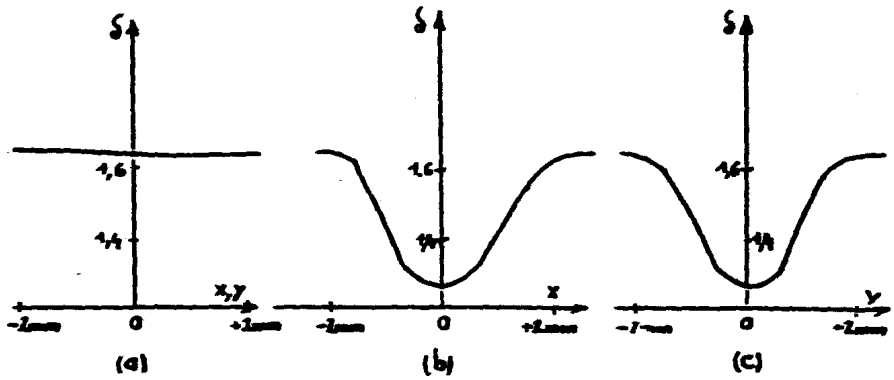

Figure 15. Variation in secondary electron emission coefficient, g, obtained by sweeping 2 mm with electron beam over a spot on which the beam had just rested for 0 minutes (a) and 100 minutes (b and c) by coworkers (Ref. 45).

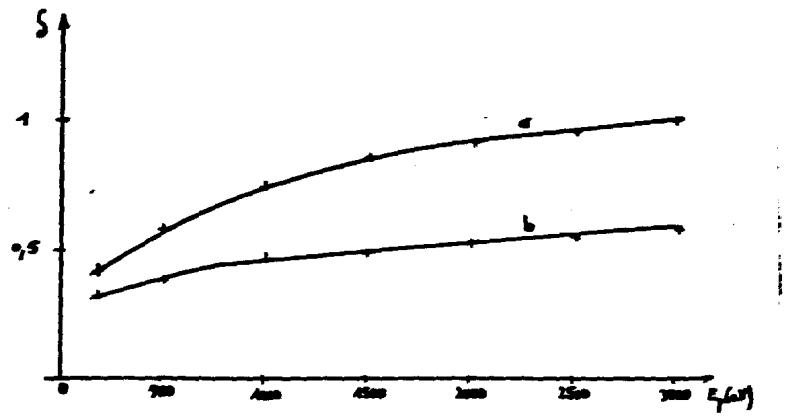

Figure 16. a)Secondary electron emission coefficients for gold black (gold soot). b)The same measurement after bombarding the material with a dose of 2×10^{20} electrons/cm^2 over a period of 110 hours - Lanarec, etc. and (Ref. 45).

V. New Coupler Designs

Since the last workshop there have been some new coupler designs as well as new work on existing designs, some of which will be briefly described here.

The fixed coupler in the Darmstadt linac is being replaced with a variable coupler having a range of $Q_{external}$ from 10^7 to nearly 10^{10} (Figure 17).[46] The new coupler is more robust and will also eliminate the problem of the external Q deviations from the desired value due to manufacturing variations. Two ceramic windows are used at 300 K with a vacuum space between them whereas the existing coupler had a window at 2 K with a second at 300 K. The coupler vacuum will be integral with the cavity vacuum and a teflon spacer at 2 K will center the probe. An interesting feature of this design is the coupling of the variable probe to an intermediate coaxial resonator centered on the beam line which greatly reduces the azimuthal field asymmetry or "coupler kick" introduced.

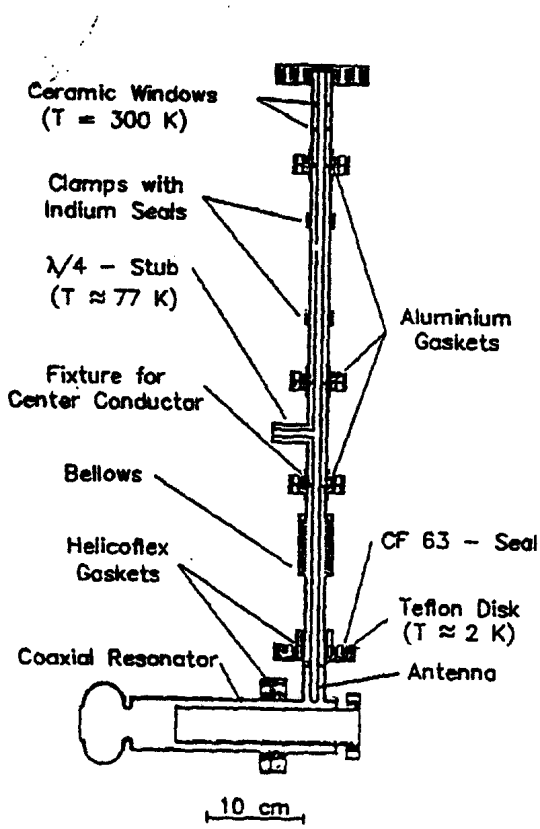

Figure 17. A newly developed coaxial coupler with variable coupling for the Darmstadt linac (Ref. 46).

The fixed coupler in LEP is also being replaced with a newly designed variable coupler.[47] The starting point is the existing LEP coupler with a bellows mounted adjustable center probe sliding through RF finger contacts. A choke is used to minimize RF current at the sliding contact. Over one hundred couplers have been produced; many have been

conditioned on the test stand to 180 KW. Two modules have new couplers installed and have been operated in the tunnel at up to 40 KW of incident power under full reflection at beam currents up to 3 ma. In general, they perform like the fixed couplers and have introduced no additional problems.

The CEBAF cold RF window consists of a thin, high purity aluminum oxide ceramic mounted in a niobium wave guide flange (Figure 18). It is sealed to the cavity fundamental power coupler port, separating the cavity vacuum from a guard vacuum maintained by a 300 K polyethylene window outside of the cryostat.

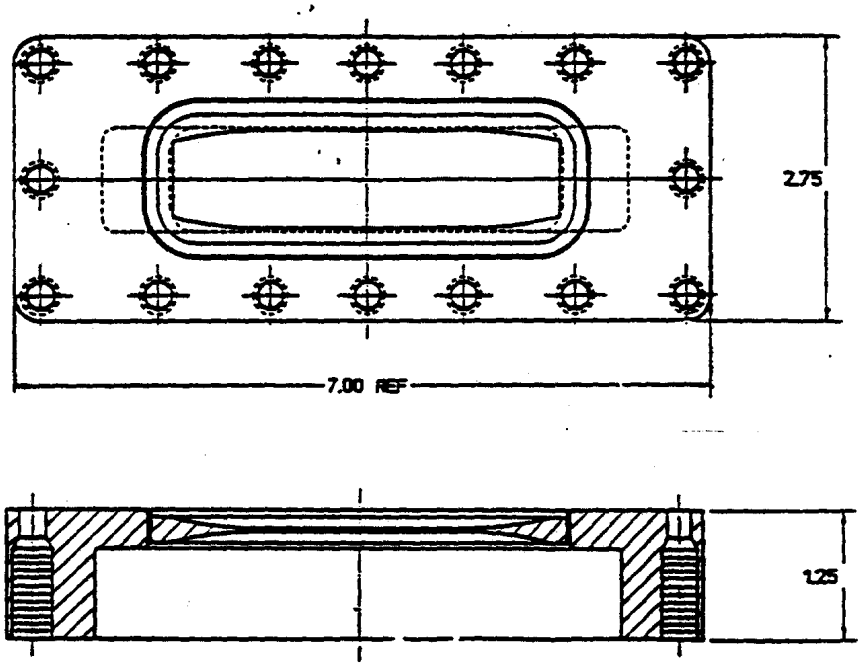

Figure 18. The CEBAF waveguide window operated at 2K.

The intent of having a window at 2 K and close to the cavity is to avoid the particulate contamination the cavity would normally be exposed to during subsequent assembly processes after leaving the clean room by attaching the window and other components necessary to seal pairs of cavities while still in the clean room.[48]. Outgassing from warm coupler parts which would also condense in the cavity during operation is also avoided. The downside of this proximity to the cavity is the increased level of electronic activity from the cavity environment as discussed earlier.

There are also a number of operating and design constraints on the window. Rejection of fundamental power (1500 MHz) in the wave guide higher order mode couplers is achieved by locating the wave guide cutoff at 1900 MHz. Higher order modes of frequency below this value must be damped by the fundamental power coupler, excluding the use of narrow band window designs. The CEBAF window uses a thin (consistent with pressure differential requirements) ceramic window filling most of the wave guide except for small irises on either side which serve to cancel the fundamental power reflection from the ceramic. The resulting VSWR is typically 1.1 at 1500 MHz and 1.3 at

1800 MHz. In order to meet the requirements of compatibility with ultra-high vacuum and cryogenic environments, a metal-ceramic design was used, the metal being primarily niobium to keep RF losses low. The only other metals used are the silver-copper braze alloy used to join the ceramic to a thin niobium transition element and the ceramic braze metallization, which in this case is an old industry standard consisting of a thin layer of molybdenum and manganese powders sintered on the ceramic surface. Typical RF loss at 2 K is 0.4 watts for 2400 watts of forward power. Most of this loss comes from the ceramic metallization. A lower-loss metallization using sputtered niobium as the ceramic bonding agent is being developed. Dielectric losses in the high purity aluminum oxide ceramic used are typically less than a few percent of the total loss.

RF windows for higher order mode couplers are not necessary for CEBAF since the HOM power is low and absorbers are located within the cavity vacuum space at the end of the HOM wave guides. This apparent simplicity imposes additional constraints on the absorber; namely, that its loss properties are adequate at 2 K and that it is UHV compatible with a low outgassing rate. The absorbers are an aluminum nitride ceramic containing glassy carbon and are brazed to a stainless steel flange (Figure 19).[49] The material used has a permittivity of 25 and loss tangents from 0.1 to 0.2 over a wide temperature range. The load exhibits return losses from 10 to 30 dB over a frequency range of 2 to 10 Ghz and the specific outgassing rate of the absorber is better than 10^{-11} torr liter/cm^2 sec.

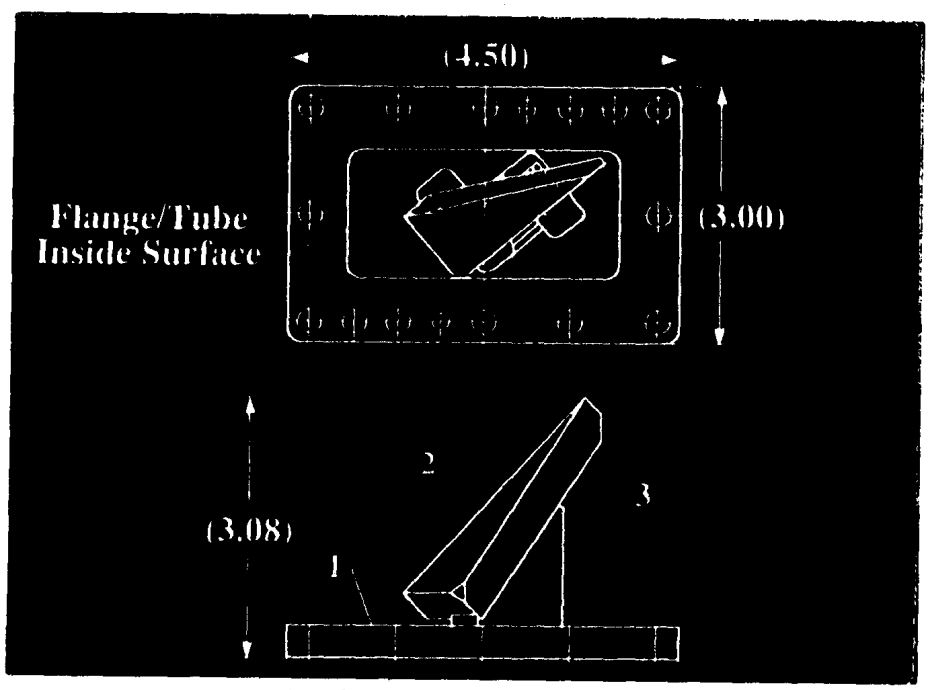

Figure 19. CEBAF HOM absorber.

Since the last workshop much effort has been devoted to the development of higher order mode propagation and absorption along the beam pipe for B-factory applications. The high beam currents of up to 2 amperes for CESR-B and low cavity impedance required, has resulted in a single cell cavity design with a layer of RF absorbing tiles of ferrite covering the inside of a section the beam pipe outside the cavity at 300K (Figure 20).[50] To ensure adequate beam stability, strong HOM damping is required, with Q's typically on the order of 100 or less. In addition to a thermal transition, a section of fluted beam pipe is placed between the cavity and the HOM load which is designed to allow unwanted

modes to propagate while maintaining a high Q for the fundamental mode.[51] (Fig. 20). The design of these cavities has been discussed in detail in a number of papers.

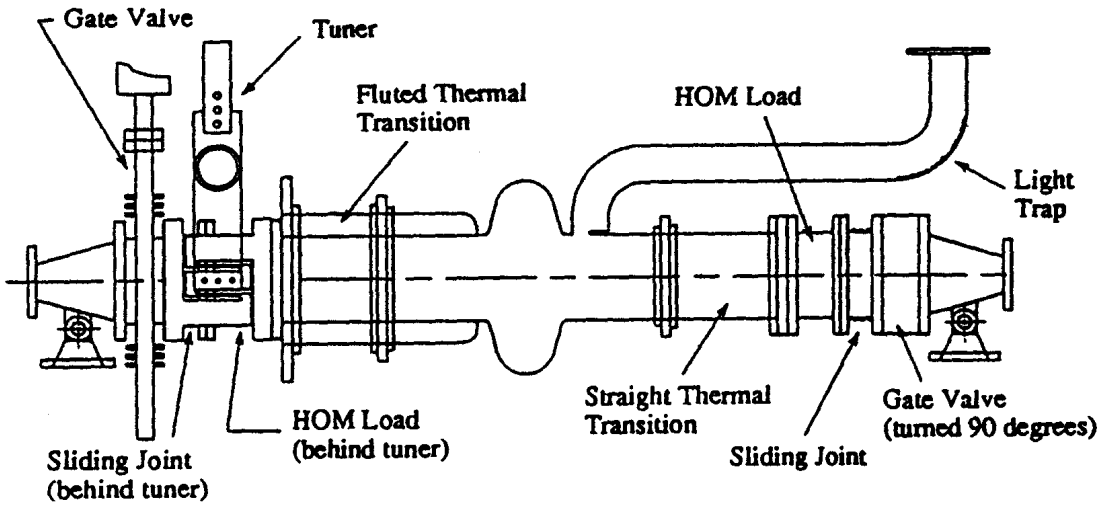

Figure 20. CESR-B cavity (Ref. 50).

One of the major technical challenges has been the design of the absorber itself. Total HOM power dissipated can be as high as 10 to 20 kW for one load with correspondingly high heat flux in the ferrite tiles.[52] The related problems of structural integrity, thermal stress cracking, UHV compatibility, and bonding of the ferrite tiles to a water jacket have been studied extensively at Cornell[53] and KEK.[54]

At Cornell good results have been obtained with a low temperature soldering process. To obtain low outgassing rates the tiles are first fired in air at 900° C after being metallized and bonded to the water cooled beam pipe with a low temperature solder. Good vacuum performance has been achieved and RF testing has been completed successfully to a power density of 10 W/cm^2.

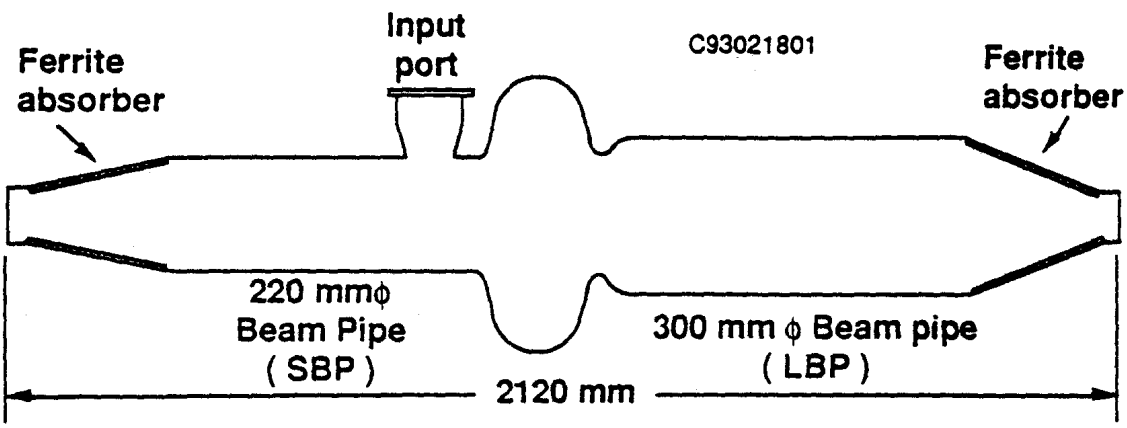

Figure 21. A KEK prototype S.C. B-factory Cavity (Ref. 55).

A parallel effort at KEK has been developing HOM loads for the KEK superconducting B-factory cavity (Figure 21).[55] Low power testing has been completed on an aluminum full scale model and HOM damping is in good agreement with calculated performance.

Work is continuing on methods of bonding ferrite tiles to a copper beam pipe. Three approaches are being explored; hot isostatically pressing the tiles or pre-sintered ferrite powder directly onto the copper, brazing, and low temperature soldering.

Vacuum brazing using silver-copper eutectic has shown some promise, and intial results bonding tiles to copper by hot isostatic pressing were good. As soon as these tests are complete, a full scale load will be made and tested in the accelerator.[56]

A prototype RF window for CESR-B was developed and tested at Cornell.[57] In this application the window is required to handle 500 kw of traveling wave power at 500 Mhz in a WR-1800 waveguide. Three beryllium oxide disks were brazed into a water cooled copper frame in reduced height waveguide on the vacuum set of the window (Figure 22).. The mismatch is tuned out by vertical posts on either side of the window resulting in the VSWR show in Figure 23. The window was tested to 260 kw of traveling wave power and was limited by vacuum bursts from wall heating which was considered to be aggravated by the additional stored energy inherent in the use of the matching posts. Work will continue on improved versions.

The TESLA coupler requirements as currently defined are a 208 kW pulsed RF power capability at 1.3 ghz for 1.33 msec at a 10 Hz repetition rate. One coupler per cavity is intended with a high-peak-power processing capability on the order of megawatt. One mechanical design complexity is the need to provide a lateral motion of up to 15 mm between the warm and cold ends of the coupler in order to accommodate the thermal contraction differential between cold and warm cryostat walls over the length of the cryostat assembly. Currently two groups in the TESLA collaboration are collaborating on parallel designs at DESY and at FERMILAB shown in Figures 24 and 25 respectively.

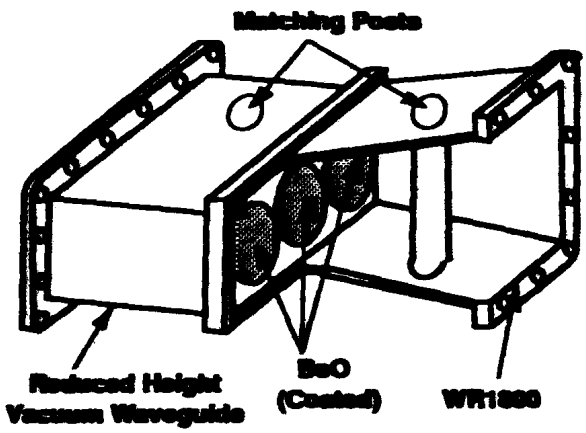

Figure 22. 500 KW, WR-1800 waveguide.

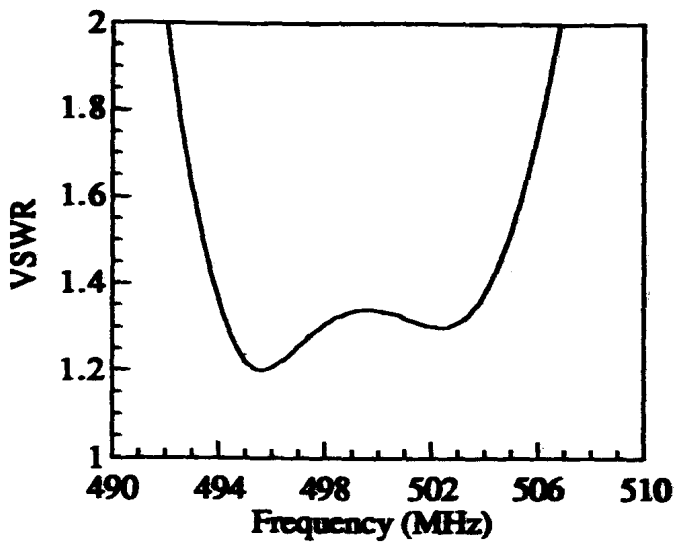

Figure 23. (Ref.57) Window for use at 500 Mhz. (Ref.57

The FERMILAB coupler[58,59] has been tested at 804 Mhz., which was the only RF source at the time, up to 1.7 megawatts at 15 Hz with a 120 μ sec pulse width. Some vacuum activity and light flashes were seen on conditioning and some steady light was

evident at specific power levels above 230 kW. The DESY design[60] has been completed and extensive field computations and shape modeling have been carried out. A prototype is under construction and will soon be RF tested. Both designs use one warm cylindrical window at the waveguide to coax transition and a second cylindrical window at the shield temperature.

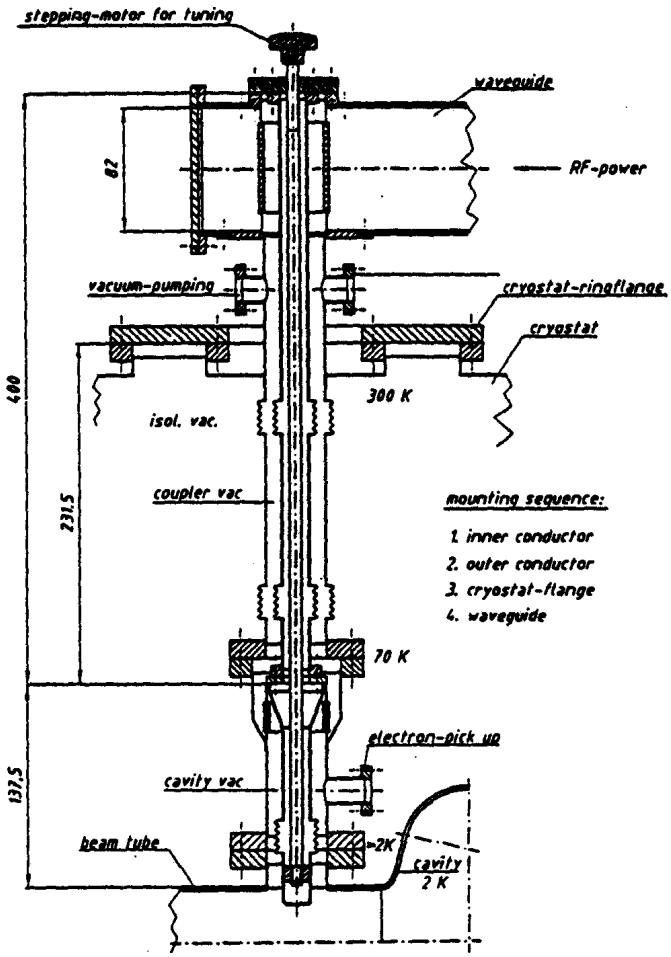

Figure 24. A TESLA input coupler design (Ref. 60).

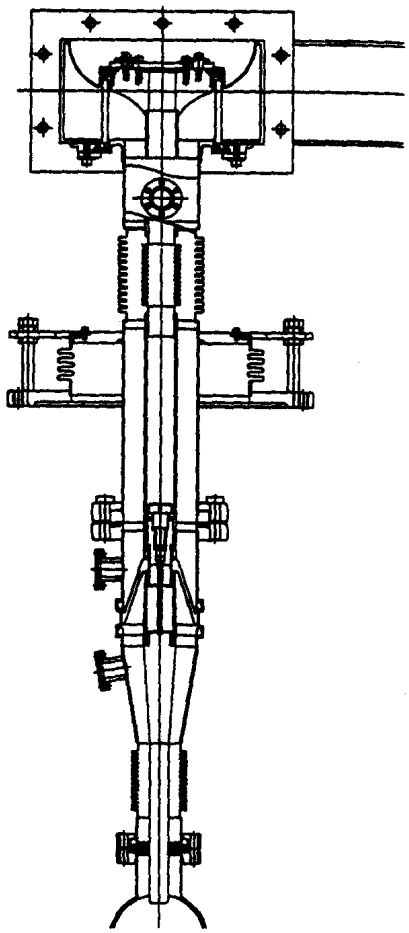

Figure 25. A TESLA input coupler design (Ref. 58.59)

Interlocks

Protective interlocks for couplers attempt to detect window arcing multipacting, or overheating. The HERA coupler diagnostic system (Figure 26) contains sensors for all of those conditions. A spark detector (photodiode) detects flashes of light from the waveguide side of the ceramic along with an infrared sensor to monitor window temperature. An additional light sensor contained in the doorknob of the waveguide to coax transition is positioned to look at the space between inner and outer conductors of the coaxial line directly into the cavity and will sense discharges in the space. Multipacting is indicated by current picked up on an electron probe biased to +30 volts

penetrating the outer conductor of the coaxial line close to the window. The LEP coupler, on which the HERA coupler is based, operates at lower power levels with a thermal interlock and a coupler vacuum interlock but without an arc detector. Coupler vacuum and coupler probe current are strongly correlated when multipacting is present, and pressure bursts in the coupler vacuum can also be used as an indication of multipacting. At KEK window arc sensors are used along with additional thermal interlocks for window cooling water and door knob temperature. An arc detector on the CEBAF waveguide coupler views light scattered from the thermal transition region between the 300 K window and a second window at the cavity. An infrared detector views basically the same region. The coupler vacuum between windows is separately pumped and interlocked but the apertures and conductances are such that the effective pumping speed of the 2 K end of the waveguide is much greater than that of the external ion pump where the pressure is measured. Mild multipacting might not be seen but significant pressure bursts are seen frequently during window/waveguide discharges. In general coupler interlocks protect both the coupler and the machine.

This has some influence on how the trip levels and response times of the interlocks are set. The procedure that tends to be followed is to observe the highest value achieved for the parameter being watched during the normal course of operation and then set the trip point somewhat higher. For the purpose of protecting the window from "sputtered" metal it is probably desirable to keep the response time of an arc interlock trigger as short as possible, since it is likely that interlocks do not entirely prevent this kind of damage but instead limit each occurrence to a small dose which eventually accumulates to a damaging level.

On the other hand the CEBAF coupler exhibits many short-lived flashes of light which do not develop into damaging "arcs" and are self-extinguishing. They do not interfere with the flow of RF power to the cavity and are masked by a time delay to avoid unnecessary interlock trips. For interlock trips beyond the time delay, the beam as well as the klystron must be turned off since the loss of one cavity will allow the beam to strike the vacuum chamber wall in an arc. If metal sputtering were a problem with this coupler, and there is no indication that it is, the arc trigger mask could be detrimental. This is not a problem at KEK since the beam is not lost until more than three klystron are switched off.

The question arises as to what interlock trips are most responsible for lost beam time. At CEBAF this is not clear yet since most trips are still caused by a variety of hardware bugs that are being uncovered and corrected. At KEK a series of trips involving the cavity quench detector, cavity vacuum, window arc sensor, and maximum field interlocks occur and the reasons are not yet fully understood. There are some patterns to their occurrence and synchrotron radiation is thought to be involved.[61] At CERN the main coupler vacuum has produced a significant number of trips. A summary of three months of luminosity runs at HERA depicted in Figure 26 indicate relatively little beam time lost due to interlock trips.[62] A breakdown of those trips by category is given in Figure 27. Four of the six categories listed are coupler related:

e^- det	—	electron probe indicating the presence of multipacting
LUVA	—	light sensor viewing the coax line interelectrode space
LUWG	—	light sensor detecting window sparks
IRWIN	—	infrared detector monitoring window temperature

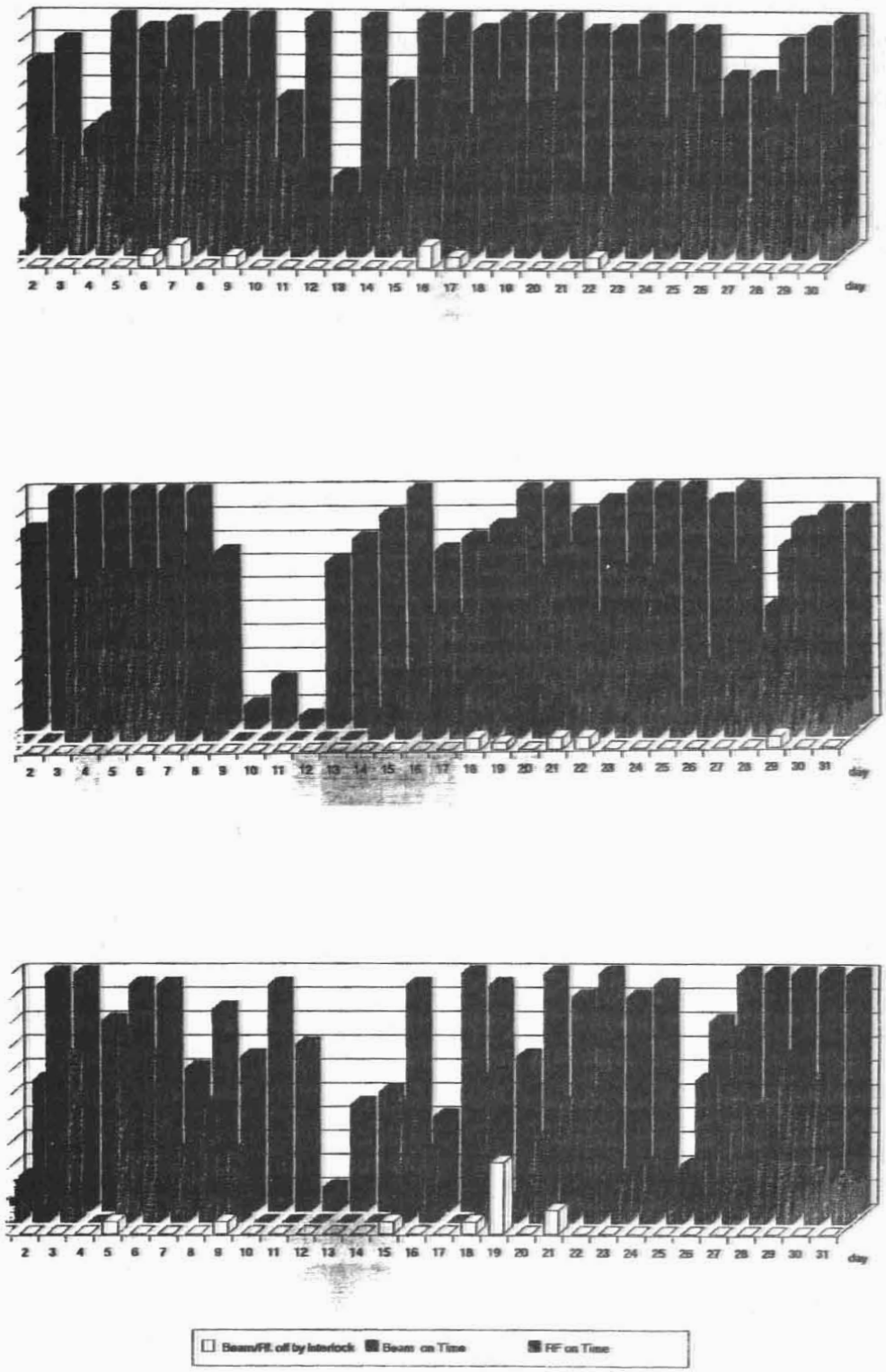

Figure 26. HERA Luminosity runs for July, August, and September, 1993 (Ref. 63).

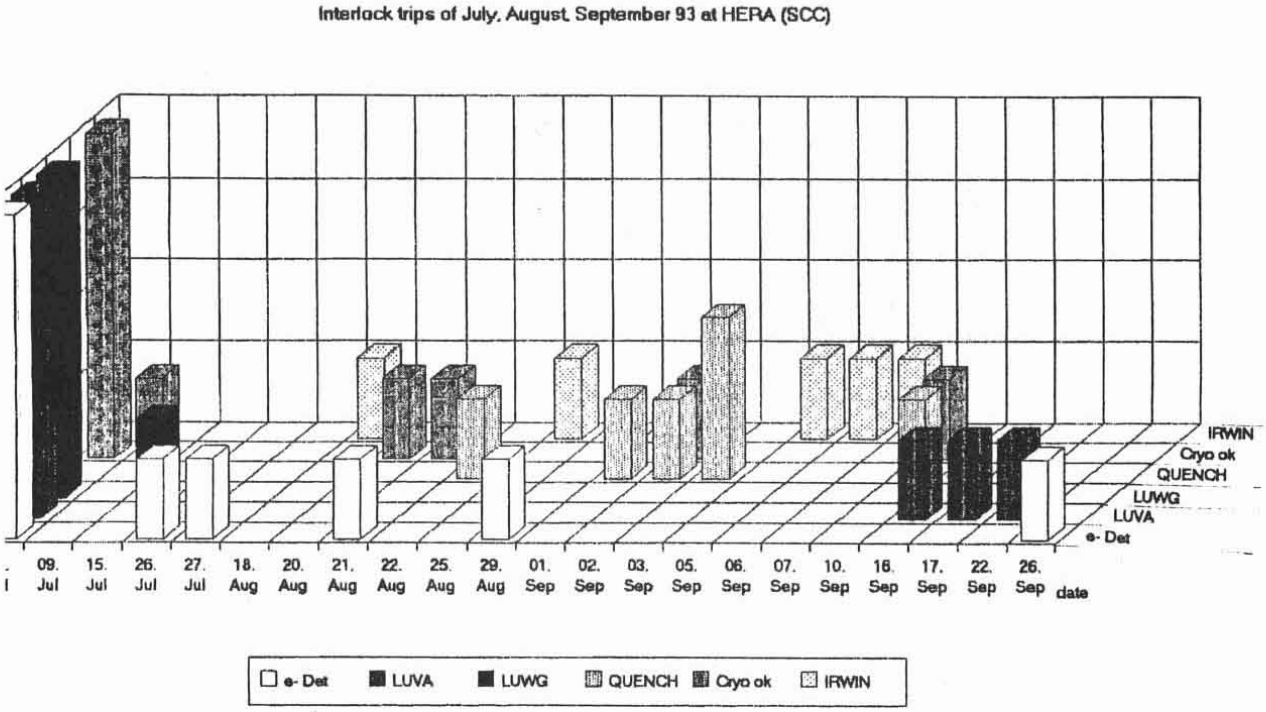

Figure 27. A breakdown of HERA interlock trips by category.

The remaining interlocks, namely QUENCH and CRYO-OK indicate and excessive helium pressure signal and low helium respectively. Although the total time lost is small, coupler trip are responsible for much of it.

Conclusions

RF window and coupler system used in superconducting RF accelerators are still limited by operational reliability problems and represent some degree of vulnerability to the accelerator. The design of these components has not been reduced to standard engineering practice to the extent that such problems can be avoided with certainty in future machines. High power klystron windows experience problems which are primarily related to defects in the ceramic material and which occur in the 50 to 200 megawatt range of peak pulsed power. SRF cavity windows exhibit multipacting and "RF sputtering" problems at much lower power levels in a totally different environment.

It is likely that RF sputtering of metals from coupler surfaces is initiated by multipacting. If this were true, nearly all SRF coupler problems could be eliminated by the suppression of multipacting. Our ability to suppress multipacting will improve significantly with improvement in our ability to measure and control the secondary electron emission coefficients of coupler surfaces in the presence of gas migration and other influences present in the accelerator environment.

Acknowledgments

The author very gratefully acknowledges his colleagues at many laboratories who provided material and valuable discussions used in this work.

*This work supported by US DOE Contract DE-AC05-84ER40150.

1 K. Hübner, "Two Beam Linear Colliders," 15th Int. Conf. on High energy Accelerators, Hamburg, July, 1992, 791.
2 H.-D. Gräf, Private communication.
3 CEBAF Design Report, May, 1986.
4 E. Kako, et al., "Long Term Performance of the Tristan Superconducting RF Cavities," IEEE Particle Accelerator Conf., San Francisco, 1992, 2408.
5 Y. W. Kang, et al., "HOM Damping with Coaxial Dampers in a Pillbox Cavity without the Fundamental Mode Frequency Rejection Filter," Proc. of the 1993 Part. Acc. Conf., 910.
6 *ibid.* 3.
7 H. Padamsee, et al., "Design Challenges for High Current Storage Rings," Proc. of the 5th Workshop on RF Superconducting, Hamburg, 1991, p 138.
8 B. Dwersteg, A. Matheisen, "15th Int. Conf. on High Energy Acc.", Hamburg, 1992, 748.
9 R. V. Latham, "High Voltage Vacuum Insulation," Academic Press, London, 1981.
10 B. C. Yunn and R. M. Sundelin, "Field Emitted Electron Trajectories For The CEBAF Cavity," Proc. of the 1993 Particl Acc. Conf., 1092.
11 F. Krienen, "Electron Wind in Strong Waveguide Fields," SLAC-PUB-3616, Mar. 1985.
12 F. Krienen, "Environmental Influences Contributing to Window Failure of the SLAC 50 MW. Klystron," SLAC AP-19, Mar. 844.
13 L. Phillips, et al., "Some Operational Characteristics of CEBAF RF Windows at 2K," Proc. of the Part. Acc. Conf., 1993, 1007.
14 Y. Saito, et al. "Breakdown of Alumina RF Window," XIIIth Int. Symposium on Discharges and Electrical Insulation in Vacuum, Paris, 1988.
15 D. Henkel and W. Hooper, "Report on CEBAF Alumina windows," CEBAF Internal Report.
16 S. Noguchi, private communication.
17 S. Noguchi, et al., 4th SRF Workshop, 1989, 397.
18 R. M. Sundelin, CEBAF TPN 91-004.
19 V. Nguyen, L. Phillips and C. Reece, to be published.
20 L. Phillips, et al., op cit 13.
21 T. Powers, et al, in proceedings of this workshop.
22 L. Phillips CEBAF TN 93-084.
23 S. Noguchi, private communication.
24 I. Ben Zvi, J. F. Crawford, and J. P. Turneaure, "Electron Multiplication in Cavities," IEEE Trans. Nucl. Sci., NS-20.
25 A. Miura and H. Matsunoto, "Development of an S-Band RF Window for Linear Colliders," Proc. of the 1993 Part. Acc. Conf., 1124.
26 R. Talcott, "The Effects of Titanium Films on Secondary Electron Emission Phenomena in Resonant Cavities and at Dielectric Surfaces," IRE Trans. on Electron Devices, 1962, p 405.
27 A. R. Nyaiesh, E. L. Garwin, F. K. King and R. E. Kirby, "Properties Of Thin Antimultipactor Coatings For Klystron Windows," SLAC-PUB-3760, 1985.
28 S. Michizono, et al., "TiN Film Coatings on Alumina Radio Frequency Windows," J. Vac. Sci. Tech. A10(4), Jul/Aug 1992, 1180.
29 A. R. Nyaiesh, op. cit. 27
30 S. Michizono, op cit. 28.
31 R. Kirby, private communication.
32 L Phillips, op. cit 13.
33 Y. Saito, et al., op cit 14.
34 A. Miura and H. Matsumoto, "Development of an S-Band High-Power Pillbox-Type RF Window," 15th Int. Conf. on High Energy Acc., Hamburg, 1992, 942.
35 Y. Saito, et al., "Surface Flashover on Alumina RF Windows for High power Use," 15th int. Symp. on Discharges and Electrical Insulation in Vacuum, Darmstadt, 1992
36 F. Krienen, "On the Coating of the SLAC Klystron Windows," SLAC/AP-23, May 23, 1984.
37 S. Michizono, op. cit. 28.
38 *ibid.*
39 L. Phillips and T. Elliott, to be published.

40 S. Anders, A. Anders, and I. Brown, "Surface Resistivity Tailoring of Ceramic Accelerator Components," Proc. of the 1993 Particle Acc. Conf., 1390.

41 R. Hayes, "Research on Microwave Window Multipactor and its Inhibition," Final Report, Contract No. DA36-039, SC-90818 Dept of the Army, Eitel-McCullough, Inc., June, 1964.

42 H. Padamsee, D. Proch, P. Kneisel, and J. Mioduszewski, "Field Strength Limitations in Superconducting Cavities-Multipacting and Thermal Breakdown," IEEE Trans. on Mdg., Vol. Mag.-17 No. 1, Jan. 1981.

43 H. Bruining, "Physics and Applications of Secondary Electron Emission," Perganon Press, New York, 1954.

44 *ibid.*

45 M. Lavarec, G. Boquet, and A. Septier, "Lowering of the Secondary Electron Emission Coefficient of Real Surfaces Due to the Primary Electron Bombardment," Proc. 8th Int. Symp. on Discharges and Elec. Ins. Vac., Albuquerque, 1978, P. C3-1.

46 H.-D. Gräf, in these proceedings.

47 E. Häebel, private communication and G. Cavallari, in these proceedings.

48 P. Kneisel, "Test of Superconducting Accelerator Structures in a Closed Vacuum System," in Proc. of 1987 Particl Acc. Conf., Washington, DC, pp. 1893-95.

49 I. Campisi, et al., "The design and Production of the Higher-Order-Mode Loads for CEBAF," Proc. of the 1993 Particle Acc. Conf., Washington, DC, 1220.

50 op cit 7

51 For CESR-B cavity design discussion see padamsee, et al., "Design Challenges for High Current Storage Rings," in 5th Workshop on RF Superconductivity, (1991), 138.

52 Op cit. 7

53 *ibid.*

54 T. Tajima, et al., "R&D on HOM Absorbers for Superconducting B-Factory at KEK," MAMA Workshop, CEBAF, 1993.

55 *ibid.*

56 See also "Development of HOM Absorbers for KEK B-Factory S C Cavities" and "Bonding of a Microwave-Absorbing Ferrite, TDK IB-004, with Copper for the HOM Damper of the KEK B-Factory SC Cavities," in these proceedings.

57 D. Metzger, et al., "Test Results and design Considerations for a 500 Mhz., 500 k Watt Vacuum Window for CESR-B," Proc. of the 1993 Part. Acc. Conf., Washington, DC.

58 M. Champion, et al., "TESLA Coupler Development," Proc. of 1993 Part. Acc. Conf., Washington, DC, 809.

59 D. Sun, et al., "High Power Test of RF Window and Coaxial Line in Vacuum," op cit., 58 p 1127.

60 B. Dwersteg, et al., "Conceptual Design of an RF Input Coupler for TESLA," 15th Int. Conf. on High Energy Accelerators, Hamburg, 1992, 954.

61 op. cit. 8

62 Noguchi, et al., "Update of the Tristan RF System," Proc. of 1993 Particle Acc. Conf. 1992.

63 D. Renken, private communication.